Modeling and Simulation of the Effect of Pressure on the Corona Discharge for Wire–plane Configuration

Nouri Hamou, Aissou Massinissa and **Zebboudj Youcef**
Laboratoire de Génie Electrique de Béjaia (LGEB).
University of Bejaia, 06000, Algeria

ABSTRACT

This paper aims to analyse the behavior of dc corona discharge in wire-to-plane electrostatic precipitators (ESP) depending on the pressure. Current-voltage curves are analyzed particularly. Experimental results show that discharge current is strongly affected by the pressure for a given atmospheric condition. Changing the values pressure does not only changes the property of the gas but also affects the corona onset conditions and ion mobility. The finite-element method is used to solve Poisson's equation and a modified method of characteristics is used to satisfy the current continuity condition. The two methods are repeated iteratively to obtain a self-consistent solution of the describing equations. We used the model which separates the corona in two distinct regions. Comparing the computed results with previously obtained experimental and calculated values tests the effectiveness of this approach. The agreement with experimental results is found to be satisfactory.

Index Terms — **Corona discharge, current-voltage characteristics, electric field, charge density, onset voltage, pressure, finite element method.**

1 INTRODUCTION

THE Electrostatic precipitators (ESP) are the most commonly employed particulate control devices for collecting fly ash emissions from boilers, incinerators and from many other industrial processes. They can operate in a wide range of gas temperatures achieving high particle collection efficiency compared with mechanical devices such as cyclones and bag filters. The electrostatic precipitation process involves several complicated and interrelated physical mechanisms: creation of a non-uniform electric field and ionic current in a corona discharge, ionic and electronic charging of particles moving in combined electro- and hydrodynamic fields, and turbulent transport of charged particles to a collection surface [1].

The ESP operates in the three-step process: charging the particles under non-uniform and very high electric field strength, collecting the charged particles on the collecting surface and cleaning the collected particles by rapping or washing the collecting electrode with a liquid. Corona discharge, as applied to electrostatic precipitators, is a gas discharge phenomenon associated with the ionization of gas molecules by high-energy electrons in a region of the strong electric field strength. The process of corona generation in the air at atmospheric conditions requires a non-uniform electrical field, which can be obtained by the use of a small diameter wire electrode and a plate or cylinder as the other electrode. An application of a high voltage to the wire results in a production of a high electric field, which reduces significantly with the increasing distant away from the surface of the wire. The reduced electric field near the collecting electrode thus helps to prevent an initiation of the electric arc or sparking due to the electron bridging across the interelectrode spaces. In contrast to the wire-plate system, a uniform electric field is generated between two parallel electrodes, which are more likely to lead to an electrical sparkover due to no limitation of electron avalanche by the reduced electric field [2-4].

Industrial ESP are used with success to reduce the emissions of smoke, fumes and dust, playing an important role to maintain a clean environment and to achieve more healthy air quality [5]. They are able to remove more than 99 % of particulates from the flue gas [6]. In these systems, particles are charged by means of the ions produced by a dc corona discharge in the common cases. The particles migrate to the collecting plate due to the Coulomb forces, but they are also under the influence of the viscous forces due to the fluid flow and ionic wind [7-10]. In such systems, the knowledge of the pressure effect on DC corona discharge behavior is of crucial importance [11]. Some effect of pressure on DC corona are not well known and requires further investigations in order to achieve realistic and valid models, which are able to be integrated in a numerical simulation.

The main objective of this investigation is to study the effect of the pressure on positive and negative corona discharge behavior in wire-to-plane electrostatic precipitator. Several design parameters were taken into consideration especially the number of active electrodes and their diameter. In particular,

Manuscript received on 3 October 2012, in final form 17 April 2013.

current-voltage curves, averaged power and onset voltage are analyzed and discussed. This paper presents a numerical algorithm which can be used to simulate the essential parameters of the process in the wires–two planes configuration, including the electric field, the space charge density and the current density.

2 EXPERIMENTAL SETUP AND PROCEDURE

The schematic representation of the wire-to-plane ESP used in this investigation is shown in Figure 1. The ESP, based on a DC corona, consisted of two parallel electrodes (stainless steel plates, 200 mm length and 100 mm width in the x-direction and z-direction, respectively). Both parallel electrodes were grounded. The high voltage electrodes consisted of a stainless steel wires with 0.2 mm of diameter and parallel to z-axis midway between the grounded electrodes. The distance between both grounded plates is equal to 100 mm.

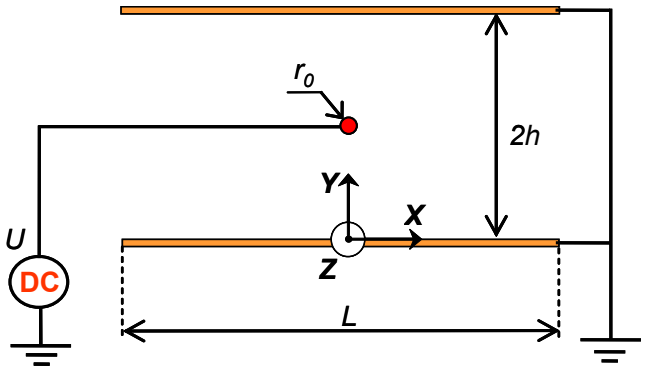

Figure 1. Electrostatic Precipitator configurations.

In this study the two DC high voltage polarities were used (positive and negative). The high voltage was applied by a DC power supply (SPELLMAN SL 150, ± 40 kV; ±3.75 mA) with an accuracy of 0.1 kV. The power supply was protected by a ballast resistor of 10kΩ. The time-averaged current was measured using a digital millimeter (METERMAN 37 XR, accuracy ≈ 1μA).

As shown in Figure 2, the experiments were carried out inside a could cylindrical vessel (glass, 500 mm-high, and 250 mm-diameter) filed with clean air. This capsule with pressure up to 5 kPa. All the pressure, temperature and humidity sensors were securely placed within the chamber through completely sealed rubber plugs. The chamber pressure was decreased from 0.1 MPa to 0.01MPa.

Since the effect of temperature on the electrical behavior of a corona discharge has been examined extensively in the literature [12, 13], the effect of pressure and the number of active electrodes were parameters taken into consideration in the present study. During each experiment, the temperature and relative humidity inside the test chamber are controlled.

Each current-voltage curves represents the average of five series of measurement. Between two of them, the gas is entirely renewed. Because the presence of corona can reduce the reliability of a system by degrading insulation. While corona is a low energy process, over long periods of time, it can substantially degrade insulators, causing a system to fail due to dielectric breakdown. The effects of corona are

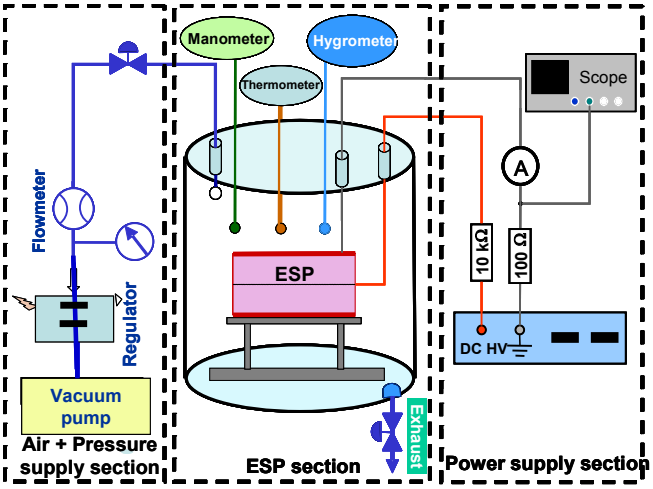

Figure 2. Experimental set up

cumulative and permanent, and failure can occur without warning (Corona causes Ozone, Nitric and various other acids).

All measurements were made in an air-conditioned laboratory; where the temperature was maintained at 22°C and relative humidity was maintained at 50% (The physical parameters of air are regularly controlled).

3 MATHEMATICAL MODELING

The solution of the space charge field for wire-duct precipitators is described in the following sections. The investigated wire-two planes configuration has a wire radius r_0 and height h above the ground plane (see Fig. 1).

The physical dimensions are wires height H = 5.0 cm, radius r_0 = 0.2 mm, with a base plane length L = 20 cm. The ion mobility was set at $\mu = 1.85\times10^{-4}$ m^2.V^{-1}.s^{-1}. The surface factor η is equal to 1.

The corona phenomenon is obtained from the following relations [7]:

$$\nabla \vec{E} = \frac{\rho}{\varepsilon_0} \quad (1)$$

$$\nabla \vec{J} = 0 \quad (2)$$

$$\vec{J} = \rho \cdot \mu \cdot \vec{E} \quad (3)$$

$$\vec{E} = -\nabla \Phi \quad (4)$$

where $\vec{E}$ is the electric field intensity vector (V/m), ρ is the space charge density (C/m^3), $\vec{J}$ is the current density vector (A/m^2), Φ is the electric potential, ε_0 is the permittivity of free space and μ is the ion mobility (1.85×10^{-4} m^2.V^{-1}.s^{-1}).

Equations (5)-(8) are, respectively, Poisson's equation, the current continuity condition, the equation of current density and the equation relating the electric field to the potential. These differential equations must be solved for the potential Φ and the space-charge density ρ, both being functions of the space coordinates.

In reality, it is extremely difficult to find an exact solution to these equations due to their nonlinear nature. However, there are analytical solutions for simple geometries such as spherical and coaxial configurations. All attempts at solving these differential equations have been based on some simplifying assumptions [14].

(i) The entire electrode spacing is filled with monopolar space-charge of the same polarity as the coronating conductor. The thickness of the ionization layer around the conductor is sufficiently small to be disregarded with respect to the interelectrode spacing.

(ii) The space-charge affects only the magnitude and not the direction of the electric field. This assumption was suggested at first by Deutsch and later referred to as 'Deutsch's assumption'.

(iii) The mobility of ions is constant (independent of field intensity).

(iv) Diffusion of ions is neglected.

(v)The surface field of the coronating conductor remains constant at the onset value E_0, which is known as Kaptzov's assumption [15]. For the conductor-to-two plane configurations, E0 is expressed in kilovolts per centimeter as:

$$E_0 = \frac{U}{h \cdot \ln\left(\frac{h}{r_0}\right)} \tag{5}$$

Where r_0 is the conductor radius in centimeters, U is the applied voltage and h is the distance between the wire and the collector plate.

The solution of equations (1)-(4), which describes the space-charge ionized field, requires three boundary conditions.

(i) The potential on the coronating conductor is equal to the applied voltage.

(ii) The potential on the grounded electrode is zero.

(iii) The magnitude of the electric field at the surface of the coronating conductor is assumed to be a function of the applied voltage.

The proposed method of analysis is described in Fig. 3. The space charge density around the periphery of the ionization region is assumed initially as:

$$\rho_{i1} = \rho_e \cdot \cos(\theta_i / 2) \tag{6}$$

Where:

$$\rho_e = \rho_0 \cdot \frac{h}{r_0} \cdot \frac{E_0}{E_{crit}} \tag{7}$$

$$\rho_0 = \frac{4\varepsilon_0 \cdot V_s \cdot (U - V_s)}{h^2 \cdot U \cdot (5 - 4 \cdot (V_s / U))} \tag{8}$$

$$E_{crit} = 30\eta[1 + (0.0906/r_0)^{1/2}] \tag{9}$$

V_s is the corona onset voltage, η is the surface irregularity factor and θ_i is the angle at which the field line emanates at the wire surface [16].

The evaluation of the space charge density for the other mesh nodes is obtained using the simplified method of characteristics which neglects ion diffusion. Ion diffusion is not considered in our work.

From the current continuity equation we can write

$$\nabla J = 0 \Rightarrow \nabla[\rho(\mu E)] = 0 \Rightarrow (\nabla\rho)(\mu E) + \rho\mu\nabla E = 0 \tag{10}$$

$$\Rightarrow \nabla\rho = \frac{-\rho^2}{\varepsilon_0 E} \quad \Rightarrow \frac{\partial\rho}{\partial r} = \frac{-\rho^2}{\varepsilon_0 E} \tag{11}$$

Integration of equation "11" gives values of the space charge density along field lines. For the resolution, we used the Runge-Kutta method [17].

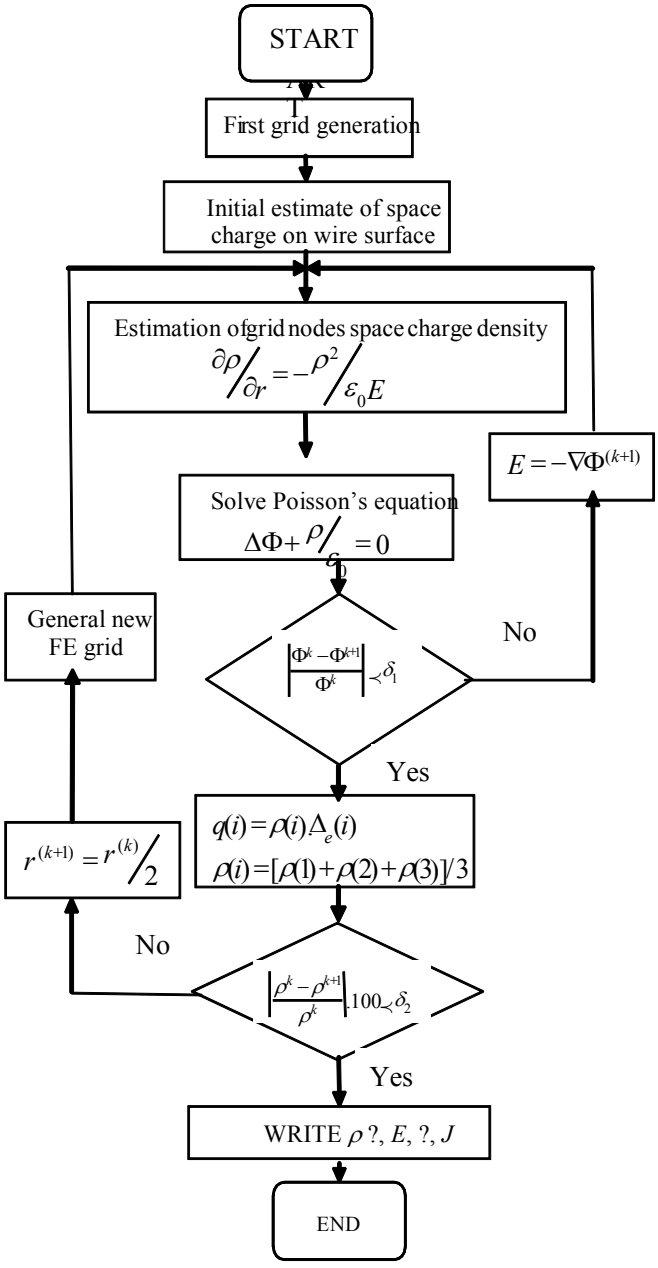

Figure 3. Flow chart of the solution method.

Using the FEM to solve Poisson's equation. The potential φ within each element is approximated as a linear function of coordinate:

$$\varphi = \varphi_1 w_1 + \varphi_2 w_2 + \varphi_3 w_3 \tag{12}$$

with 1, 2, and 3 representing the nodes of the element e, and w is the corresponding shape function [18, 19].

A functional Re is for mulcted in the usual FEM:

$$R^e = -\int_A [W]^T \left[\left(\frac{\partial \varphi}{\partial x} \right)^2 + \left(\frac{\partial \varphi}{\partial y} \right)^2 + \frac{\rho}{\varepsilon_0} \right] dA \tag{13}$$

where A is the area of triangular element, $[W]$ is the row vector containing the elements shapes functions.

Equation (11) is transformed into linear equation by minimizing the functional Re, in the form:

$$[K].[\Phi] = \{F\} \tag{14}$$

Where:

$$[K] = \sum_{e=1}^{Elt.Num} k_{ij}(e) \tag{15}$$

$$\{F\} = \sum_{e=1}^{Elt.Num} f_i(e) \tag{16}$$

$$k_{ij} = \iint_{\Delta_e} \left[\frac{\partial N_i}{\partial x} \cdot \frac{\partial N_j}{\partial y} + \frac{\partial N_i}{\partial y} \cdot \frac{\partial N_j}{\partial x} \right] \cdot dxdy \tag{17}$$

$$f_i = \sum_n \iint_{(e_i)_n} \frac{\rho_i}{\varepsilon_0} \cdot N_i \cdot dxdy \tag{18}$$

$$N_i(x,y) = \frac{1}{2 \cdot \Delta_e} (a_i + b_i x + c_i y) \ , i = 1, 2, 3 \tag{19}$$

Note that $N_i(x_j, y_j)$ is the shape function and the coefficients of a_i, b_i and c_i can be easily determined from the definition of the shape function in the finite element theory.

4 RESULTS AND DISCUSSION

4.1 THE CURRENT-VOLTAGE CHARACTERISTICS

Figures 4 and 5 show the current-voltage characteristics obtained with the ESP for both voltage polarities.

The ionization process by a collision is the basis for gas multiplication. The number of electron-ion pairs created by a single electron drifting a unit distance in the field direction in a gas is denoted as the first Townsend coefficient α of the gas. It depends principally upon the nature of the gas, the gas pressure, and the electric field intensity.

The pressure increase causes a variation of the ionization coefficient α, in the ionization region, and a variation of the ion mean free path length λ, in the drift region, for a fixed potential voltage value U between the electrodes.

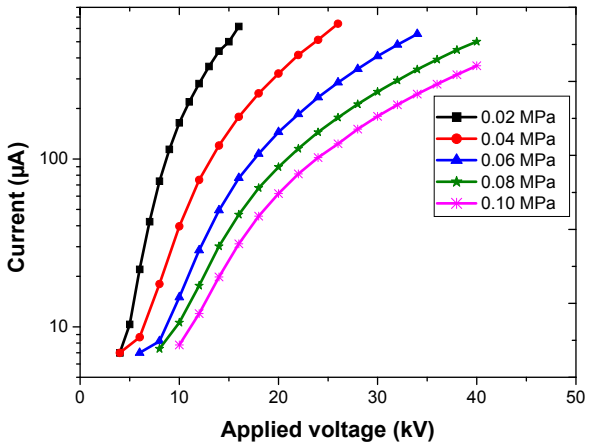

Figure 4. Current-voltage characteristic of negative corona.

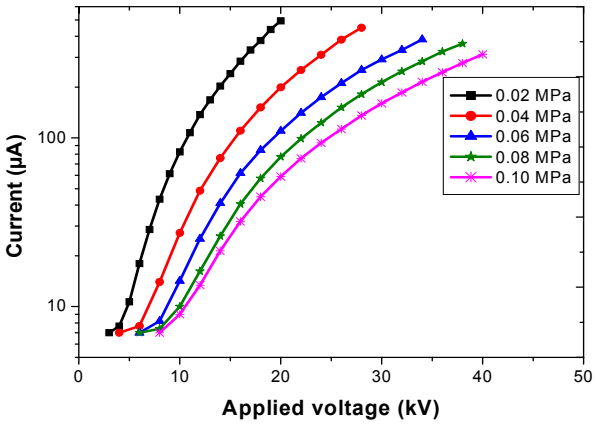

Figure 5. Current-voltage characteristic of positive corona.

The ionization and attachment coefficients can well be represented by the equations of the type [20, 21]:

$$\alpha/p = A \exp\left[-B\left(p/E \right) \right] \tag{20}$$

$$\eta/p = C + D\left(E/P\right)^2 + F\left(E/P\right) \tag{21}$$

Where p is the atmospheric pressure in Pa and E the electric field in V.cm^{-1}. The constants A, B, C, D and F are determined by curve fitting the experimental results on ionization and attachment data [22].

It is assumed that the transport properties of the air are determined by E/N, where E is the local electric field and N is the neutral gas density. For most real gases, p can be directly measured whereas N cannot, we often quote the quality E/p in place of E/N (N is the number of molecules in unit volume).

As the pressure goes up, α decreases, thus producing a lower ionization rate close to the tip. As a consequence, the current generated by the corona discharge decrease. The sequence of phenomena at 0.02 and 0.04 MPa gas were essentially the same as at 0.1 MPa, except that the threshold potentials were correspondingly lower to Corona onset voltage.

4.2 CORONA ONSET VOLTAGE

Figure 6 shows the evolution of Vs against the pressure for both high voltage polarities and the two ESP designs.

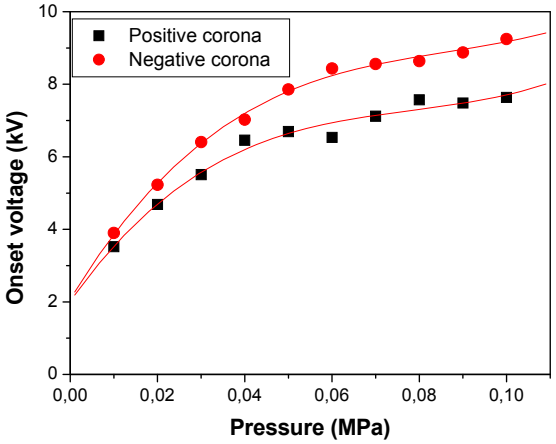

Figure 6. Variation of corona onset voltage with pressure.

By applying correction factors, a discharge voltage measured in given test conditions, may be converted to the value that would have been obtained under the standard reference atmospheric conditions. Therefore we have:

$$V_{0p} = \delta . V_s \tag{22}$$

Where δ is the air density correction factor. V_s is the onset voltage at standard reference atmosphere.

When the temperatures T and T_0 are expressed in degrees Celsius and the atmospheric pressures p and p_0 are expressed on the same units (kPa or mbar), the relative air density is:

$$\delta = \left(\frac{p}{p_0}\right)\left(\frac{273+T_0}{273+T}\right) \tag{23}$$

The onset voltage values are entirely experimental, and the values injected in our model in order to get a best convergence. The voltage- pressure curves represent the average of five series of measurements. The time-averaged current is measured through a digital multimeter (METERMAN 37 XR) and a digital oscilloscope (Lecroy 424, 200 MHz, 2 GS/s) in same time.

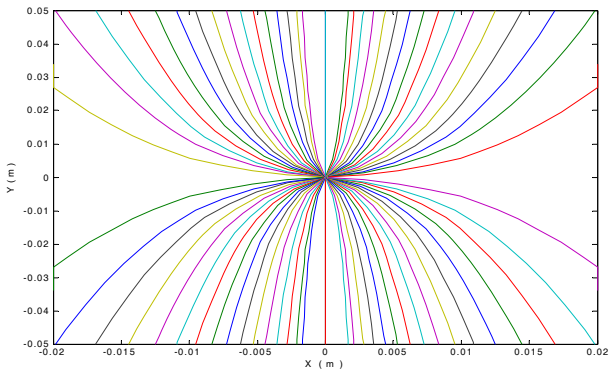

Figure 7. Field lines.

4.3 GENERATED GRID FOR A PRECIPITATOR

Figure 7 show characteristic lines for the system of wire-plate geometry with operating voltage of 20 kV and p = 0,1 MPa.

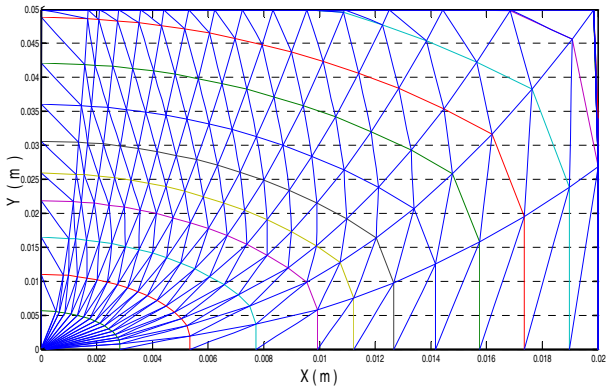

Figure 8. Generated grid for a precipitator.

The grid is generated from the intersection of field lines with equipotential contours see Fig.8. This is called field mapping.

4.4 ELECTRIC FIELD

The distribution of electric field is shown in Figs. 9 and 10.

This investigation describes the process of an electric field production in an ESP. When ESP is used for gaseous applications, ions are produced by high voltage electric input.

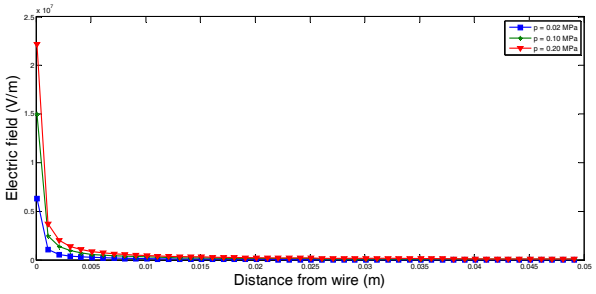

Figure 9. Variation of electric field with pressure (U = 20 kV).

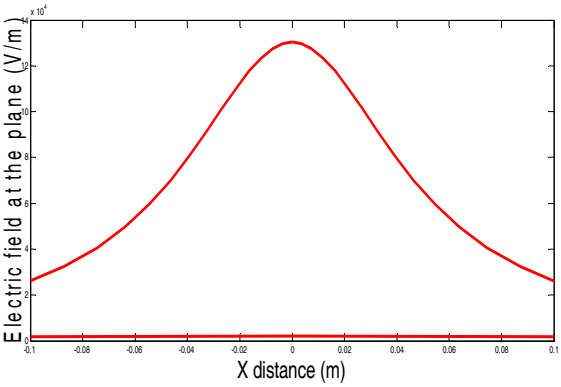

Figure 10. Electric field distribution at the plane (U = 20 kV and p = 0.1 MPa).

4.5 CURRENT DENSITY AT THE GROUND PLANE

The calculated and experimental distributions of current density at the ground plane are shown in Figures 11 and 12.

The purpose of this paper is to report our investigations of corona discharge in electrostatic precipitator, either positive or negative polarity. The corona discharges were generated in a plasma reactor between two electrodes. The results of the measurements are compared with the numerical simulation obtained. The comparison was made in terms of the current density.

The 2D simulation performed in this paper can only approximate the electric field in the given configuration. An accurate calculation would require the use of 3D models. Though the calculation of Laplace electric field in 3D arrangements poses no essential problem by any of the existing numerical methods, the accurate description of the actual geometry would require a very tedious work and this effort was considered to be beyond the scope of this paper.

The present finite element algorithm is applied and compared to the most recent previous work which adopted the FET. The FE grid is generated in a simple way with the characteristic lines following the FE grid pattern. This simplicity is due to the way by which the FE grid is generated.

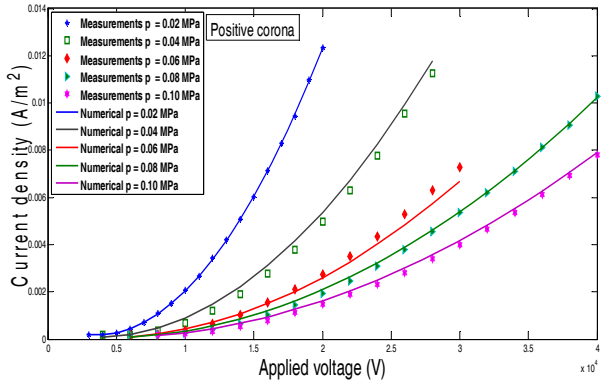

Figure 11. Current density distribution at the plane for positive corona.

Corona discharge occurs when the voltage applied to the thin electrode is high enough to ionize the gaseous species surrounding the discharge electrode.

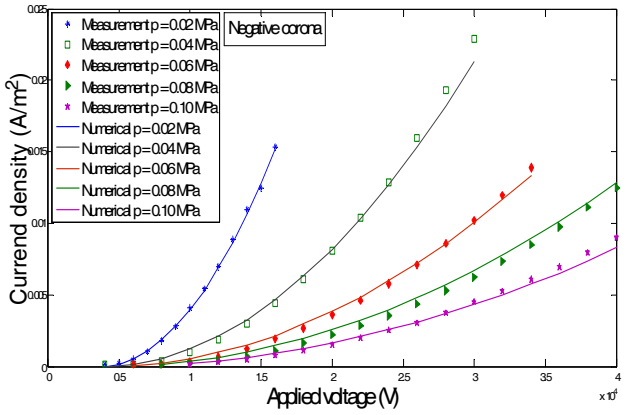

Figure 12. Current density distribution at the plane for negative corona.

The results will advance the knowledge of corona discharge at low atmospheric pressure. The discharge type is strongly dependent on the atmospheric pressure. The glow discharge is frequently observed at lower pressure. The corona inception volume decreases with the decrease in atmospheric pressure. The electrostatic filter can be operated even at low voltages by reducing the pressure. For p = 0.01 MPa for example, a voltage more than 2 kV is sufficient to ionize the particles using an electrode with 0.2 mm in radius. For the same conditions and using a pressure of 1 bar, the air ionizes starting from a voltage of 12 kV. By changing the pressure, therefore the optimum operating conditions change. So, we will be in the obligation to determine the relationship between the pressure and voltage in order to ensure the best functioning of the system.

5 CONCLUSION

In the present work, in this paper, the effect of pressure on a DC corona discharge behavior in wire-to-plane electrostatic precipitator has been investigated. The onset voltage is proportional to the increase of pressure.

The finite element method is shown to be uniformly applicable to all the equations describing the problem of electric field in corona devices. Using the Newman and Dirichlet boundary conditions method enables quadratic convergence of steady-state solutions such that they are obtained in a few steps.

The proposed numerical computation takes into account the thickness of the ionization region, whereas previous works of this problem ignored this parameter. We integrate the potential correspondent to the minimum ionization field directly in the formulation of the FEM on the border of the ionization region, which reduces the algorithm computation.

The experimental results were compared with existing theories. The agreement between the calculated values of electric field, space charge density and current density and those obtained experimentally is satisfactory.

REFERENCES

[1] S.H. Kim and K.W. Lee, “Experimental study of electrostatic precipitator performance and comparison with existing theoretical prediction models”, J. Electrostatics, Vol. 48, pp. 3-25, 1999.

[2] L. Zhao and K. Adamiak, “EHD flow in air produced by electric corona discharging in pin-plate configuration”, J. Electrostatics, Vol. 63, pp. 337-350, 2005.

[3] M. Abdel-Salam and Z. Al-Hamouz, “Analysis of Monopolar Ionized Field as influenced by Ion Diffusion”, IEEE Trans. Industry Applications, Vol. 31, No. 3, pp. 484-493, 1995.

[4] P. Saiyasitpanich, *Control of Diesel Particulate and Gaseous Emissions using a Single-stage Tubular Wet Electrostatic Precipitator*, Ph.D. Thesis, University of Cincinnati, Cincinnati, Ohio, USA, 2006.

[5] A. Mizuno, "Electrostatic precipitation", IEEE Trans. Dielectr. Electr. Insul., Vol. 7, pp. 615-624, 2000.

[6] J. S. Chang, "Next generation integrated electrostatic gas cleaning systems", J. Electrost., Vol. 57, pp. 273-291, 2003.

[7] T.Yamamoto and H. R. Velkoff, "Electrohydrodynamics in an electrostatic precipitator”, J. Fluid Mech., Vol. 108, pp. 1–18, 1981.

[8] P. Atten and F.M.J. Mccluskey, A.C. Lahjomri, "The electrohydrodynamic origin of turbulence in electrostatic precipitators", IEEE Trans. Ind. Appl., Vol. 23, pp. 705–711, 1987.
[9] J. Podliński, J. Dekowski, J. Mizeraczyk, D. Brocilo and J. S. Chang, "Electrohydrodynamic gas flow in a positive polarity wire-plate electrostatic precipitator and the related dust particle collection efficiency", J. Electrostat., Vol. 64, pp.259-262, 2006.
[10] N. Zouzou, B. Dramane, P. Braud, E. Moreau and G. Touchard, "EHD flow in DBD precipitator", Int'l. J. Plasma Environmental Sci. Technology, Vol.3, No. 3, pp. 142-145, 2009.
[11] K. R. Parker, *Applied Electrostatic Precipitation,* Edition Kluwer Academic Publishers, London, 1997.
[12] C. G. Noll, "Temperature dependence of dc corona and charge-carrier entrainment in a gas flow channel", J. Electrostatics Vol. 54, pp. 245–270, 2002.
[13] P. N. Mikropoulos, C. A. Stassinopoulos and B. C. Sarigiannidou, "Positive Streamer Propagation and Breakdown in Air: the Influence of Humidity", IEEE Trans. Dielectr. Electr. Insul., Vol. 15, No. 2, pp. 416 – 425, 2008.
[14] M. Abdel-Salam and Z. Al-Hamouz, "Analysis of Monopolar Ionized Field as influenced by Ion Diffusion", IEEE Trans. Industry Applications, Vol. 31, No. 3, pp. 484-493, 1995.
[15] N. A. Kaptzov, *Elektricheskie invlentiia v gazakh i vakuumme*, OGIZ, Moscow, pp. 587-630, 1947 (in Russian).
[16] K. Adamiak, "Adaptative approach to finite element modelling of corona fields", IEEE Trans. Industry Applications, Vol. 30, No. 2, pp. 387-393, 1994.
[17] H.J. Lee and W.E. Schiesser, *Ordinary and partial differential equation routines in C, C++, Fortran, Java, Maple and Matlab*, Chapman & Hall/CRC press company, pp. 20–113, 2004.
[18] H. Nouri and Y. Zebboudj, "Analysis of positive corona in wire-to-plate electrostatic precipitator". European Phys. J., Appl. Phys., Vol. 49, No. 11001, 2010.
[19] E. Kuffel, *High Voltage Engineering*, Pergamon Press, Oxford, UK, pp. 266-277, 1984.
[20] R. Benocci, M. Urbano and L. Mauri "Study of a positive corona discharge in argon at different pressures", Europ. Phys. J. D, Vol. 37, pp. 115-122, 2006.
[21] B. S. Rajanikanth and B. R. Prabhakar, "Modeling of Prebreakdown VI Characteristics of a Wire-plate Electrostatic Precipitator Operating under Combined dc-pulse Energization", Vol. 1, No. 6, pp. 1058 -1067, 1994.
[22] K.Yamazaki and R.G. Olsen, "Application of a Corona Onset Criterion to Calculation of Corona Onset Voltage of Stranded Conductors", IEEE Trans. Dielectr. Electr. Insul., Vol. 11, No. 4, pp. 674-680, 2004.

H. Nouri was born in Algeria. He received the Ph.D. degree in electrical engineering, from Bejaia University, Algeria in 2010. He is currently an associate professor in the department of electrical engineering, Setif University. His research interests are the application of corona discharge, non – thermal plasma technology and air pollution control. Dr. Nouri is a member of Laboratoire de Génie Electrique of the University A. Mira of Bejaia.and French society of electrostatics.

A. Massinissa was born in Bejaia, Algeria, in 1977. He received the Electrical Engeneering degree from Bejaia University of Science and Technology in 2002. and the Magister degree from Bejaia University of Science and Technology in 2005 discussing a thesis on corona effects in HVDC lines. From 2005 he is Member of the laboratory of high voltage of Bejaia.

Y. Zebboudj is Professor at the University A Mira of Béjaia (Algeria). He received the Ph.D. degree from the University P. et M. Curie (Paris) in 1988. He is the director of the Laboratoire de Génie Electrique of the University A. Mira of Bejaia. He is the author of many publications on corona discharge. He is the one of pioneers who established the generalized Peek's law.